RHEUMATOLOGY

Rheumatology 2022;61:4952–4961
https://doi.org/10.1093/rheumatology/keac078
Advance Access publication 14 February 2022

Original article

Defining imaging sub-phenotypes of psoriatic arthritis: integrative analysis of imaging data and gene expression in a PsA patient cohort

Lihi Eder [1,2,3], Quan Li[4], Sara Rahmati[5], Proton Rahman[6], Igor Jurisica[5,7,8] and Vinod Chandran [2,3,5,6,9]

Abstract

Objectives. To define imaging sub-phenotypes in patients with PsA; determine their association with whole blood gene expression and identify biological pathways characterizing the sub-phenotypes.

Methods. Fifty-five patients with PsA ready to initiate treatment for active disease were prospectively recruited. We performed musculoskeletal ultrasound assessment of the extent of inflammation in the following domains: synovitis, peritenonitis, tenosynovitis and enthesitis. Peripheral whole blood was profiled with RNAseq, and gene expression data were obtained. First, unsupervised cluster analysis was performed to define imaging sub-phenotypes that reflected the predominant tissue involved. Subsequently, principal component analysis was used to determine the association between imaging-defined sub-phenotypes and peripheral blood gene expression profile. Pathway enrichment analysis was performed to identify underlying mechanisms that characterize individual sub-phenotypes.

Results. Cluster analysis revealed three imaging sub-phenotypes: (i) synovitis predominant [$n = 31$ (56%)]; (ii) enthesitis predominant [$n = 13$ (24%)]; (iii) peritenonitis predominant [$n = 11$ (20%)]. The peritenonitis-predominant sub-phenotype had the most severe clinical joint involvement, whereas the enthesitis-predominant sub-phenotype had the highest tender entheseal count. Unsupervised clustering of gene expression data identified three sub-phenotypes that partially overlapped with the imaging sub-phenotypes suggesting biological and clinical relevance of these sub-phenotypes. We therefore characterized enriched differential pathways, which included: immune system (innate system, B cells and neutrophil degranulation), complement system, platelet activation and coagulation function.

Conclusions. We identified three sub-phenotypes based on the predominant tissue involved in patients with active PsA. Distinct biological pathways may underlie these imaging sub-phenotypes seen in PsA, suggesting their biological and clinical importance.

Key words: ultrasound, imaging, psoriatic arthritis, spondyloarthritis, gene expression

BASIC SCIENCE

Rheumatology key messages

- Cluster analysis defined three imaging sub-phenotypes: synovitis-predominant; enthesitis predominant; and peritenonitis predominant.
- Imaging clusters partially overlapped with gene expression signatures, reinforcing their biological and clinical relevance.
- Differential pathways underlying imaging sub-phenotypes included immune system, complement system, platelet activation and coagulation function.

[1]Rheumatology Division, Women's College Research Institute, Women's College Hospital, [2]Rheumatology Division, Department of Medicine, [3]Institute of Medical Science, [4]Princess Margaret Cancer Centre, University Health Network, University of Toronto, [5]Schroeder Arthritis Institute, Krembil Research Institute, University Health Network, Toronto, ON, [6]Rheumatology Division, Department of Medicine, Memorial University, St. John's, NL, [7]Departments of Medical Biophysics and Computer Science, Faculty of Dentistry University of Toronto, ON, Canada, [8]Institute of Neuroimmunology, Slovak Academy of Sciences, Bratislava, Slovakia and [9]Department of Laboratory Medicine and Pathobiology, University of Toronto, ON, Canada

Submitted 29 September 2021; accepted 7 January 2022

Correspondence to: Lihi Eder, Women's College Research Institute, Room 6326, Women's College Hospital, 76 Grenville Street, Toronto, Ontario M5S 1B2, Canada. E-mail: lihi.eder@wchospital.ca

Introduction

Clinical, radiological and molecular heterogeneity is a hallmark of PsA as musculoskeletal inflammation can affect different tissues including the synovial joint, tendons, entheses, bursae and bone [1, 2]. This in turn is reflected in a variety of clinical and imaging features and disease courses, which raises the question whether the extent and the severity of involvement of each tissue is determined by unique pathogenetic mechanisms or if there is a common overarching pathogenic cause.

Several lines of evidence support potential variability in the underlying immunologic pathways that govern the diverse manifestations of PsA. Prior work has shown a considerable genetic heterogeneity in the PsA phenotype where certain HLA-class I alleles play a role in determining distinct features of the disease [3–5]. Furthermore, differential expression of circulating protein mediators of various immune pathways that correlated with PsA phenotype was reported [6]. Immunologic heterogeneity was suggested to underlie differences in response to biologic therapies among patients with PsA [7]. Collectively, these preliminary data support the existence of genetic/immunologic heterogeneity underlying the various PsA disease sub-phenotypes.

The inherent inaccuracy of clinical musculoskeletal examination is one of the major challenges that hampers the study of PsA sub-phenotypes [2, 8]. This limitation has prompted the use of imaging modalities, primarily musculoskeletal ultrasound, to evaluate various manifestations of PsA. Imaging phenotyping could improve the precision of evaluating the extent of disease process in relevant target tissues in PsA (e.g. joint, enthesis, tendon, peritendon). This approach has been successfully applied in research of neurologic disorders, where obtaining tissue from target organs is challenging [9, 10]. However, to date this approach has been only infrequently used in PsA.

The objective of this proof-of-concept study was to define integrative sub-phenotypes in PsA: first, use imaging that reflects the predominant tissue/structure involved; second, determine the association between imaging defined sub-phenotypes and whole blood gene expression; and third, identify specific biological pathways characterizing the sub-phenotypes.

Methods

Setting and patients

Consecutive patients with PsA who were ready to initiate treatment for active peripheral musculoskeletal disease were prospectively recruited from two academic clinics in Toronto, Canada. The inclusion criteria were: (i) a rheumatologist-confirmed diagnosis of PsA and satisfying the classification criteria for psoriatic arthritis (CASPAR) criteria [11]; (ii) active musculoskeletal inflammation in one or more peripheral sites including tendon, joint or enthesis; and (iii) intent to initiate systemic treatment to manage active PsA including non-steroidal anti-inflammatory drug or biologic and non-biologic disease-modifying antirheumatic drugs (DMARDs). The exclusion criteria were (i) pure axial PsA with no peripheral involvement; and (ii) current use of biologic DMARDs or systemic corticosteroids. The patients were assessed clinically by a rheumatologist, ultrasound and laboratory tests were performed within 1 week of the clinical assessment.

The study was approved by the Research Ethics Board of Women's College Hospital (REB #2013–0052-E). All patients have provided written informed consent at the time of study entry.

Collected clinical data

All patients were evaluated by an experienced rheumatologist according to a standard protocol, independently of the imaging data. The following variables were recorded: demographics, medications, BMI, tender and swollen joint count in 68 and 66 joints, respectively, number of dactylitic digits, number of tender entheseal sites by SPARCC [12], psoriasis area and severity index, psoriatic nail lesions, CRP.

Imaging phenotyping using musculoskeletal ultrasound

Ultrasound was used to objectively quantify the extent of inflammation and its distribution across the various peripheral tissues involved in PsA. A comprehensive musculoskeletal ultrasound assessment was performed by a single experienced sonographer (L.E.) according to a standard protocol. A MyLab Twice (Esaote, Genova, Italy) scanner equipped with a 6–18 MHz linear array transducer was used. Power Doppler settings were standardized with a Doppler frequency of 8.3–10 MHz (depending on body habitus), pulse repetition frequency of 750 Hz, and a wall filter of 2. A systematic greyscale (GS) and power Doppler (PD) examination of 64 joints, 24 tendon sites and 16 entheses in the upper and lower extremities was performed (see Supplementary Table S1, available at *Rheumatology* online). Each site was scanned initially in longitudinal plane and any abnormality detected was confirmed in transverse plane. Each scan was recorded and stored as a short video file for later reading. Images were read and scored by a single reader (L.E.) who was blinded to the clinical information.

Sonographic inflammation in four domains was scored and graded according to validated instruments [13–15]. The following domains were scored: synovitis, peritenonitis, tenosynovitis, enthesitis. Synovitis was defined as the presence of synovial hypertrophy in B-mode and intra-articular PD and graded on a scale of 0–3 in GS and PD [13]. Peritenonitis, peri-tendon inflammation in the extensor tendons in the fingers and toes, was graded in GS as normal = 0 and abnormal = 1 and in PD as 0 = none, 1 = mild, 2 = moderate, 3 = severe [16]. Tenosynovitis, synovial inflammation in tendons with tendon sheath was evaluated in the flexor fingers,

extensor tendons in the wrist and the tibialis posterior tendon. Tenosynovitis was graded from 0 to 3 in GS and PD [14]. Enthesitis was scored only for inflammatory sonographic lesions in GS and PD, including the following lesions: hypoechogenicity (0–1), thickening (0–1) and PD (0 = none, 1 = mild, 2 = moderate, 3 = severe) [15].

The following global inflammatory scores were calculated for each tissue domain as the sum of scores from all joint/tendon/entheseal sites: synovitis score (0–384), peritenonitis score (0–224), tenosynovitis score (0–84), enthesitis score (0–80). Intra-rater reliability of ultrasound scoring was assessed by having the sonographer re-score 10 sets of stored ultrasound scans (>1 year after the first scoring). Intra-rater reliability was excellent with an intra-class correlation coefficient of 0.90 across all domains.

Whole blood RNA sequencing

Whole blood RNA was collected during the clinic visits and stored at −80°C until the analysis. Total RNA was used to create a sequencing library to provide gene-level expression of >20 000 targets covering >95% of human RefSeq genes. TopHat (v2.1.1) package [17] was used to align the RNA reads in raw FASTQ files using human hg19 genome as reference. Quality controls were done using FASTQC (Simon Andrews, http://www.bioinformatics.babraham.ac.uk/projects/fastqc/) and RSeqQC [18]. Cufflinks tool (version 2.2.1) [19] was used to quantify the gene expression in each sample as fragments per kilobase of transcript per million mapped reads, and then normalized within-sample to transcripts per million (TPM) reads. All data were transformed as log2(TPM + 1). Differentially expressed genes (DEGs) were detected using limma (3.38.3) package [20]. The heatmap and hierarchical clustering were generated using the ComplexHeatmap R package [21]. Euclidean distance with Ward's minimum variance method were used for hierarchical clustering. Principal component analysis (PCA) and plot were performed using R.

Statistical analysis

Continuous data were described by the medians (interquartile range) and categorical variables were expressed as frequencies and percentages. An important issue is that there is little interest to define clusters based on the extent of disease activity alone; therefore, we aimed to investigate whether different clusters may be defined based on the relative contribution of the involved domain. Data input to the cluster analysis included ultrasound scores with normalized inflammatory scores for each domain. We used the relative size of the total scores for each domain derived by dividing the total score in each domain by the total number of sites involved (total number of tendons, joints and enthesis with GS and/or PD score of >0). We preformed unsupervised cluster analysis to identify imaging sub-phenotypes of PsA based on sonographic continuous scores. All variables were standardized before the clustering analysis (mean 0, SD. 1). To determine the optimal number of clusters, we performed hierarchical cluster analysis and reviewed plots using varying number of clusters ($n = 2$–8). We identified three as the optimal number of imaging clusters based on the degree of separation and using the 'elbow method' with total within-cluster sum of square. In this 'elbow method', we plotted the explained variance against the number of clusters. Then, the optimal number of clusters was obtained by the elbow point where increasing the number of clusters does not bring a significant change in the explained variance [22]. The clinical and imaging parameters were compared between the three imaging clusters using the Kruskal–Wallis test for continuous variables and Fisher's exact test for categorical variables.

Gene expression and network and pathway analysis

DEGs were identified by comparing each of the three imaging clusters to the remaining two clusters (total three comparisons, $P < 0.05$, Fold change >1.2). We subsequently performed PCA of transcript data and plotted by imaging cluster.

To identify genes that are characteristic of each cluster/sub-phenotype, we found the overlap of DEGs identified after pairwise comparisons. Because none of the detected differentially expressed genes survived multiple hypothesis correction, we used an integrative computational biology approach. To identify biologically relevant differential genes, we used physical protein interactions and pathway data. We hypothesized that if the identified differentially expressed genes play a role in rewiring of signalling pathways between any two clusters/sub-phenotypes, their protein products must be physically connected. Therefore, for each comparison we first mapped genes with fold change of at least 1.4 and raw *P*-value <0.05 to the physical protein-protein interaction (PPI) network obtained from Integrative Interaction Database ver. 2020–05 (http://ophid.utoronto.ca/iid) [23], i.e. network 'seeds'. Next, we expanded the identified list to genes whose protein products have direct PPIs with seeds and their fold change is at least 1.2 (regardless of *P*-value), i.e. differential level 1 neighbours, and direct PPIs with protein products of level 1 neighbours whose fold change (FC) is at least 1.2 (regardless of *P*-value), i.e. level 2 neighbours. We performed pathway enrichment analysis using core pathways in pathDIP ver. 4 (http://ophid.utoronto.ca/pathDIP) [24] to characterize pathways enriched with extended list of differential genes in each comparison. These pathways were next manually grouped by human experts (L.E., P.R., V.C.) into eight representative categories. Network was visualized using NAViGaTOR ver. 3.0.16 [25].

Results

A total of 55 patients with active PsA were included in the study (median age 47 years, 49.1% females). Most

patients had early disease (median of 1 year since PsA diagnosis) and were mostly naïve to any DMARDs (52.7%) and to biologic DMARDs (96.4%). Seventeen patients (30.9%) were using non-biologic DMARDs at the time of assessment and none of the patients was on biologic DMARDs at that time (Table 1).

Definition of imaging sub-phenotypes

Cluster analysis identified three as the optimal number of clusters (Fig. 1). The standardized total scores in the enthesitis, synovitis and peritenonitis domains differed significantly between the three clusters.

Cluster 1 (C1, $n = 33$), the largest cluster, was characterized by high synovitis scores and low scores in the remaining domains ('synovitis-predominant sub-phenotype'). Cluster 2 (C2, $n = 13$) was characterized by high enthesitis scores and low tenosynovitis, enthesitis and peritenonitis scores ('enthesitis-predominant sub-phenotype'); and Cluster 3 (C3, $n = 11$) was characterized by high peritenonitis scores and moderate synovitis, enthesitis and tenosynovitis scores ('peritenonitis-predominant sub-phenotype').

Distribution of domain-specific inflammation by site in each imaging sub-phenotype

The distribution of the various imaging domains by clusters is depicted in Fig. 2. Enthesitis was most prevalent in the enthesitis (C2) and peritenonitis (C3) predominant clusters, with a generally equal distribution between the knees, elbows and Achilles' tendon (20–30% of the entheses affected). In contrast, enthesitis was much less frequent in the synovitis cluster (affecting <10% in most entheseal sites). Peritenonitis was almost exclusively affecting the peritenonitis cluster, predominantly affecting the fingers. Similarly, tenosynovitis was predominantly affecting the peritenonitis cluster, most commonly affecting the first to third fingers and wrist and was less frequent in the other clusters. Synovitis affected all clusters, predominantly affecting the wrists, metacarpophalangeal joints, knees and toes, but the highest prevalence of affected joints was found in the peritenonitis cluster.

Clinical characteristics of the imaging sub-phenotypes

The characteristics of the study population by cluster/sub-phenotype are shown in Table 1. There were no differences in the demographics, PsA duration and psoriasis characteristics between the three clusters. The primary differences across clusters were in the severity of clinical joint and entheseal involvement. The peritenonitis-predominant sub-phenotype was characterized by polyarthritis and moderate degree of clinical enthesitis. The synovitis-predominant sub-phenotype was characterized by oligoarthritis and minimal clinical enthesitis. The enthesitis-predominant sub-phenotype was characterized by the presence of clinical enthesitis in the majority of the patients.

Gene expression and pathway analysis by imaging clusters

The distinct biologic basis of the imaging-based sub-phenotypes was suggested by the distinct gene expression profiles of the imaging clusters as shown in Fig. 3. Principal component analysis of DEG data identified three clusters that partially overlapped with the imaging clusters. A clear separation was noted between the peritenonitis-predominant cluster and the enthesitis-predominant cluster, while the synovitis-predominant cluster partially overlapped with both clusters.

A total of 125 genes were differentially expressed across the three imaging clusters. Seventy-six genes

Table 1 Clinical features by imaging clustering

Variable	Cluster 1: synovitis predominant ($n = 31$)	Cluster 2: enthesitis predominant ($n = 13$)	Cluster 3: peritendonitis predominant ($n = 11$)	All ($n = 55$)
Age (years)	45 (20)	47 (14)	49 (16)	47 (19)
Sex: female	15 (48.4%)	8 (61.5%)	5 (45.5%)	27 (49.1%)
PsA duration (years)	0.8 (3.7)	1.2 (1.5)	1.6 (11.5)	1 (4)
Age at diagnosis of psoriasis (years)	26 (33)	37 (26)	39 (20)	31.5 (30)
Age at diagnosis of PsA (years)	42 (22)	45 (19)	44 (18)	44 (20)
BMI (kg/m^2)	26.1 (8.4)	29.4 (6.8)	25 (8.1)	26.2 (8.5)
Presence of nail lesions	**17 (54.8%)**	**3 (23.1%)**	**5 (45.5%)**	**25 (45.5%)**
PASI	2.8 (7.8)	1.2 (2.7)	1.2 (3.2)	1.5 (6)
Tender joint count	**3 (6)**	**6 (9)**	**11 (5)**	**5 (9)**
Swollen joint count	**3 (6)**	**2 (6)**	**10 (7)**	**4 (7)**
Presence of dactylitis	7 (22.6%)	3 (23.1%)	4 (36.4%)	14 (25.5%)
Presence of clinical enthesitis	**15 (48.4%)**	**12 (92.3%)**	**7 (63.6%)**	**34 (61.8%)**
Enthesitis count	**0 (2)**	**3 (3)**	**1 (4)**	**1 (3)**
CRP (mg/l)	3.6 (9.4)	2.9 (8.8)	8.5 (21.5)	3.7 (10.1)

Bolded if statistically different between the three groups (two-sided $P < 0.05$).

Fig. 1 Hierarchical clustering of patients based on musculoskeletal ultrasound (MSK-US) based tissue-level inflammation data

Figure 1 – Hierarchical clustering of imaging data based on tissue-level inflammation

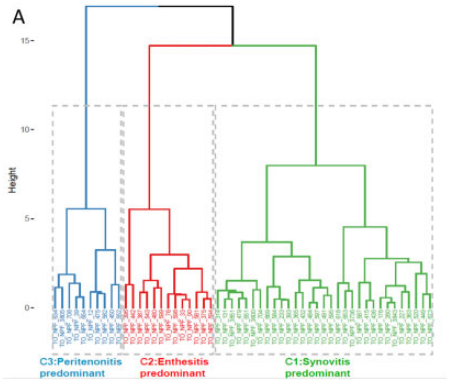

1B. Standardized Ultrasound Scores by Imaging Cluster (median and IQR)

	Cluster 1 Synovitis predominant (N=31)	Cluster 2 Enthesitis predominant (N=13)	Cluster 3 Peritenonitis predominant (N=11)	P value
Synovitis score	1.86 (0.64)	1.15 (0.34)	1.59 (1.40)	0.004
Enthesitis score	0.24 (0.34)	0.83 (0.19)	0.50 (0.45)	<0.001
Peritenonitis score	0.29 (0.70)	0.13 (0.27)	1.13 (0.22)	<0.001
Tenosynovitis score	0 (0.39)	0 (0.27)	0.27 (0.43)	0.59

*Standardized scores= total sonographic score in the domain divided by the total number of affected articular/tendon/entheseal sites

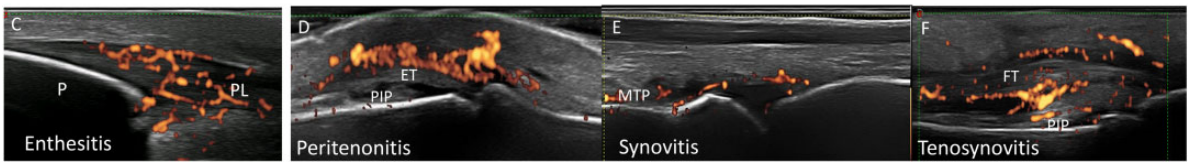

(**A**) Hierarchical clustering identified three clusters. (**B**) MSK-US scores of the four domains evaluated by imaging cluster. (**C**)–(**F**) Images demonstrating inflammation in the four domains. (**C**) Enthesitis in the patellar ligament. (**D**) Peritenonitis of the extensor digitorum tendon. (**E**) Synovitis of the metatarsophalangeal joint. (**F**) Tenosynovitis of the flexor digitorum tendon.

Fig. 2 Distribution of domain-specific inflammation by site in each imaging sub-phenotype

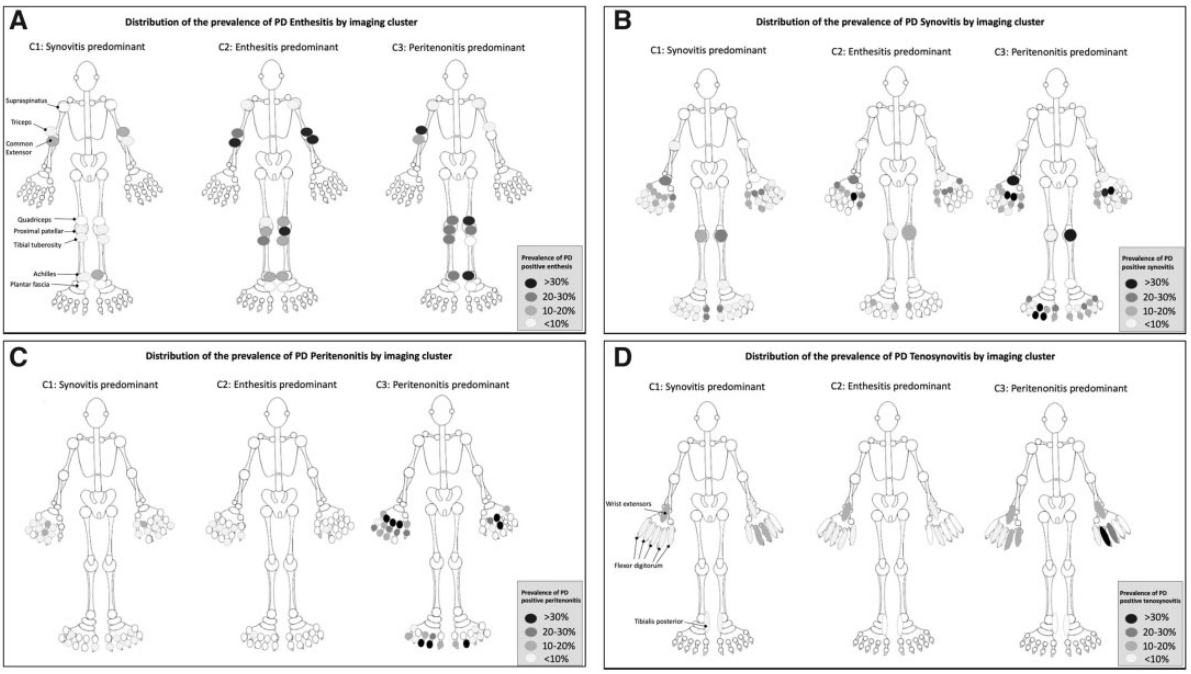

FIG. 3 Gene expression pattern by imaging clusters

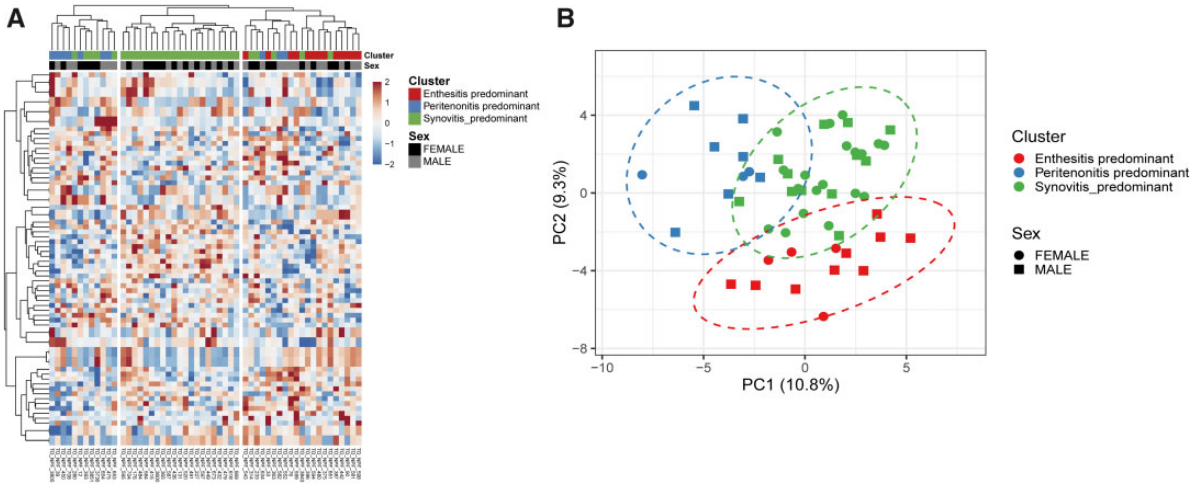

(**A**) Heatmap of DEG by imaging clusters. (**B**) PCA by imaging clusters.

characterize the synovitis-predominant sub-phenotype; 30 genes are characteristic of the peritenonitis-predominant sub-phenotype, and 19 genes distinguished the enthesitis-predominant sub-phenotype from the other two sub-phenotypes; however, no gene was differentially expressed in all three comparisons and comprehensive pathway analysis also failed to identify any significantly enriched pathways.

We attribute this lack of enrichment to insufficient statistical power of the DEG analysis due to small sample size. For this reason and to provide biological relevance, we used a network-based approach with physical protein interactions and pathways. First, we connected DEGs by considering physical interactions of protein products (available in PPI networks). To 'seed' the network, we only considered genes with raw $P < 0.05$ and FC > 1.4. Second, we kept only their network neighbors with FC > 1.2. This resulted in 383 DEGs between enthesitis and peritenonitis, 237 DEGs between enthesitis and synovitis, and 256 DEGs between peritenonitis and synovitis (complete list of DEGs is available upon request). Next, we performed pathway enrichment analysis using these DEGs (see Supplementary Fig. S1, available at *Rheumatology* online). To help interpretation, we then grouped enriched pathways into eight major categories and highlighted the most frequent genes across pathways and within specific pathway categories (Fig. 4).

Pathways related to the immune system (innate system and neutrophil degranulation), complement system, platelet activation and degranulation and coagulation function were found to underlie many of the DEGs between the three sub-phenotypes, with most of the DEG being those belonging to the immune system category. Most of the pathways were those distinguishing between the synovitis-predominant *vs* enthesitis-predominant and peritenonitis-predominant *vs* enthesitis-predominant sub-phenotypes, suggesting that the enthesitis-predominant sub-phenotype has more distinct underlying pathways that are different than the other two clusters. Another notable difference between the synovitis and enthesitis sub-phenotypes was expression of genes related to B-cell activation pathways.

Discussion

The mechanisms driving clinical heterogeneity in PsA remain largely unexplained. In this study we used imaging-based clustering to answer the question whether heterogeneity in PsA arise from different pathogenetic mechanisms or whether there is a common overarching pathogenic cause. We identified three partially overlapping imaging sub-phenotypes that were characterized by their predominant tissue involved, and were termed accordingly: synovitis-predominant, enthesitis-predominant and peritenonitis-predominant. Additionally, using gene expression and pathway analysis we found that distinct pathogenic pathways including innate immunity, neutrophil function, coagulation, complement and platelet activation may underlie some of the heterogeneity seen in PsA, characterizing these three sub-phenotypes.

Unlike other inflammatory rheumatic conditions, in which a single biologic marker, such as serologic test (e.g. anti-citrullinated peptide antibody) or genetic test (HLA-B*27), helps classify most patients, PsA is a spectrum of disease, classified predominantly using clinical findings. Based on the CASPAR criteria, the presence of psoriasis and negative test for rheumatoid factor can be sufficient for classifying a patient with inflammatory arthritis as PsA [11]. This clinically driven disease classification is expected to result in significant heterogeneity in the underlying pathogenic causes, clinical presentation and consequently variability in natural history and treatment response. Attempts to classify patients with PsA into subtypes, including the classification by Moll and

Fig. 4 Pathway enrichment results

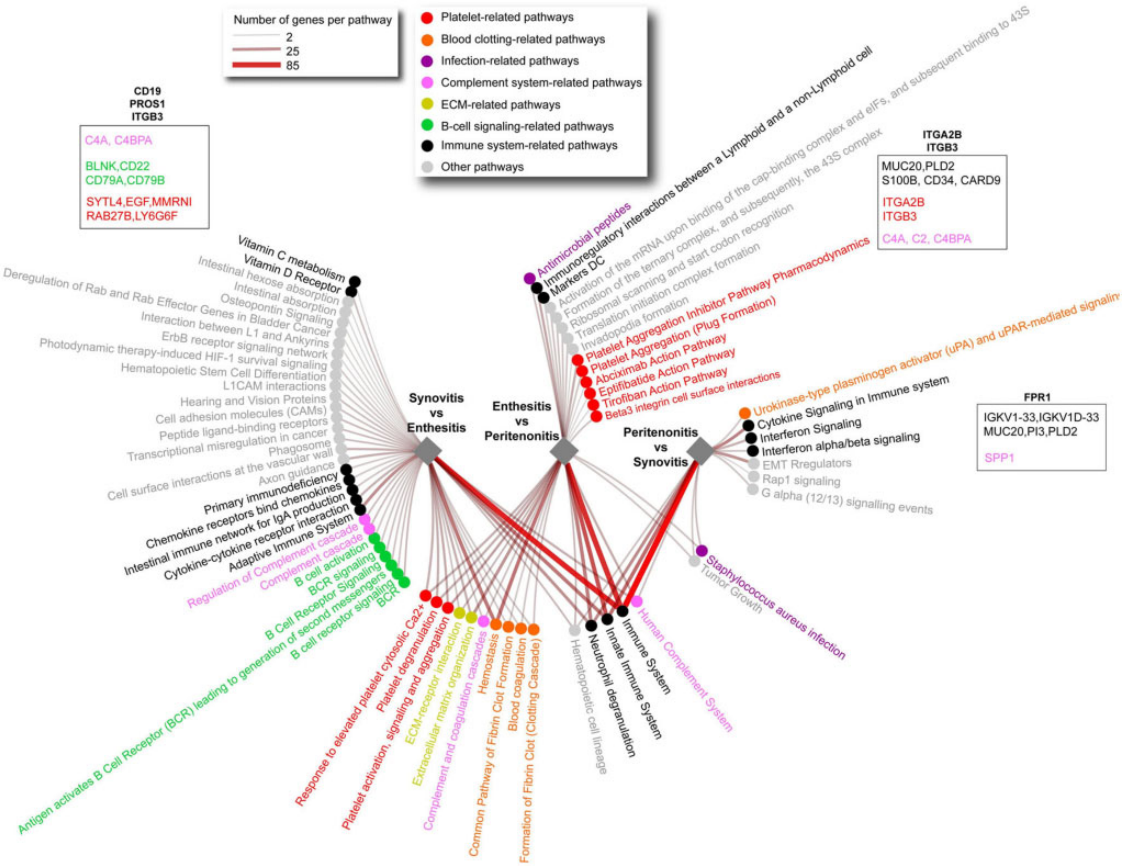

To address the small sample size and to provide biological relevance, we used physical protein interactions to connect DEGs to other genes with FC >1.2. We then performed pathway enrichment analysis using the extended DEGs and to improve interpretability, we grouped enriched pathways into eight major categories, colour-coded as per the legend. Edge thickness corresponds to number of genes within the pathway, and the most frequent genes across set of pathways are highlighted in bold text, while the genes most frequent in a specific category of pathways are colour-coded as per the legend (placed inside the text boxes).

Wright [26], were based for the most part on clinical features, such as polyarthritis *vs* oligoarthritis and axial *vs* peripheral involvement. This type of clinical-based classification was restricted by the inherent limitations of physical musculoskeletal examination, especially when considering the entheses and tendon involvement, and calls for the use of musculoskeletal imaging for studying PsA phenotypes. In this context, our study provides a novel disease insight by exploring the heterogeneity of tissue-specific inflammatory involvement in PsA.

Several important findings emerge from our study. First, patients could be classified to partially overlapping clusters/sub-phenotypes by their predominant tissue involved, despite the frequent co-occurrence of inflammation in several domains. These sub-phenotypes were indistinguishable in many of the clinical and demographic features, but varied in their gene expression signatures, adding to the validity of this clustering and highlighting the added value of imaging in studying PsA pathophysiology.

Second, despite being a characteristic feature of PsA, extra-articular inflammation does not affect all patients. PsA is characterized by the combination of intra-articular (synovitis) and extra-articular inflammation (peritenonitis, enthesitis, tenosynovitis). However, our study showed that while synovitis affected all clusters, extra-articular inflammation varied significantly across clusters. Synovitis-predominant sub-phenotype, the largest cluster affecting over half of patients, was characterized by low prevalence of extra-articular inflammatory features. Enthesitis-predominant sub-phenotype was characterized by high enthesitis scores but low peritenonitis. Peritenonitis, inflammation of tendons without a synovial sheath, as in the extensor tendons of the fingers and toes, is a unique characteristic of PsA. Peritenonitis distinguishes patients with PsA compared with rheumatoid arthritis and it has been hypothesized to be a form of 'functional enthesitis' [27]. In our study, the peritenonitis-predominant sub-phenotype was characterized by most active disease with moderate-high scores across all

domains; it also had highest levels of total tender and swollen joint count and CRP levels; thus, suggesting that peritenonitis may be considered an imaging marker of more severe PsA.

Importantly, we have found an association between gene expression signatures and imaging clusters supporting the notion that different biological pathways may underlie disease presentation. Previous research into the pathogenic mechanisms underlying PsA clinical features identified few potential sources. Genetic studies have shown that HLA-B*27 was associated with sonographic enthesitis [28] and axial involvement [4] while HLA-B*08 was associated with synovial-based features including joint deformity and fusion [3]. Sokolova *et al.* showed that the IL-17 induced proteins, beta-defensin-2 and lipocalin-2, were associated with a subset of patients with enthesitis while products of innate immune system activation and neutrophil activation were associated with a subset of patient with peripheral arthritis [6].

Further, we were able to identify several pathways that may play a role in PsA heterogeneity using physical protein interaction networks and comprehensive pathway enrichment analysis. We found that in addition to genes belonging to the immune system, component of the coagulation cascade along with platelet function contributed to the heterogeneity in PsA presentation. The role of platelets and the coagulation cascade in cardiovascular disease is well established. However, while these pathways may drive the increased cardiovascular risk in PsA, their contribution to the inflammatory process is less understood. Activated platelets can elicit immune response either directly by secretion of inflammatory mediators, such as calprotectin, or indirectly through their interaction with other effector immune cells, such as neutrophils [29]. Emerging data support the potential role of platelets in psoriasis. Platelets were detected in psoriatic skin but not in heathy skin; they often colocalize with polymorphonuclears, platelet surface antigens characterize psoriasis polymorphonuclears, and the depletion of platelets improved psoriasiform lesions in mice [30–32]. In addition, biomarkers indicating activation of the coagulation cascade and vascular damage have been associated with more active psoriasis and PsA [33, 34]. Overall, abnormalities in platelet and the coagulation function have been described in psoriatic patients and may drive heterogeneity in disease presentation; however, the exact nature of this association requires further research.

Our study was limited in several aspects. Firstly, the small sample size may have limited our ability to detect distinct pathways driving the individual imaging clusters and to validate the clustering method in an independent cohort. The small sample size and the lack of longitudinal clinical data also precluded us from assessing the value of these clusters in predicting important clinical outcomes. Secondly, the presence of axial involvement was not evaluated but it may contribute to PsA heterogeneity. However, it has been suggested that MRI confirmed axial involvement affects only a small proportion of PsA patients [35]; therefore, the lack of spine imaging data is not expected to significantly modify the results. Thirdly, we analysed whole blood RNA expression; tissue-specific (e.g. synovial) or cell specific (e.g. T cell) expression may provide more clear differences across groups. Finally, we evaluated patients at a single timepoint, and it is unclear whether the imaging clusters remain stable over time and whether they predict treatment outcomes.

Our study had several important strengths that include a comprehensive phenotyping of the extent of musculoskeletal inflammation in relevant domains using imaging, which is more accurate than clinical assessment. Our study also included patients with early disease onset and active PsA who were not using biologic DMARDs at enrolment. This is expected to reduce the heterogeneity of the study population and minimize biases occurring due to concurrent treatments. By performing protein interaction network and pathway enrichment analyses, we provide stronger biological context to our findings.

In summary, we identified three partially overlapping imaging sub-phenotypes that were characterized by their predominant tissue involved and characterize the heterogeneity seen in PsA. Distinct biological pathways involving immune and non-immune pathways may underlie the different features in PsA and support the validity of this imaging clustering. Additional research is needed to characterize the functional link between imaging clusters and disease course and treatment outcomes.

Acknowledgements

L.E. is Canada Research Chair (Tier 2) in Inflammatory Rheumatic Diseases (2021–2026) and is supported by the Early Researcher Award from the Ontario Ministry of Research, Innovation and Science. I.J. was supported in part by funding from Natural Sciences Research Council (NSERC #203475), Canada Foundation for Innovation (CFI #225404, #30865), Ontario Research Fund (RDI #34876), IBM and Ian Lawson van Toch Fund. V.C. is supported by a Pfizer Chair Research Award, Rheumatology, University of Toronto, Canada.

Funding: The study was supported by a Discovery grant from the National Psoriasis Foundation. The funders had no role in study design, data collection and analysis, decision to publish, or preparation of the manuscript.

Disclosure statement: L.E. received research grants/research support from Abbvie, Eli Lily, Janssen, Novartis, Pfizer, UCB and consultation fees from Novartis, Eli Lily, Janssen, Abbvie, Pfizer. P.R. received grants/research support from Janssen, Novartis and consultation and speaking fees from Abbvie, Amgen, BMS, Celgene, Pfizer, Novartis. V.C. received grants/research support from Abbvie, Celgene and consultation fees from Abbvie, Amgen, BMS, Celgene, Eli Lily, Janssen, Novartis, Pfizer, UCB; employment of spouse: Eli Lily. The other authors declare no conflicts of interest.

Data availability statement

Data are available upon reasonable request by any qualified researchers who engage in rigorous, independent scientific research, and will be provided following review and approval of a research proposal and Statistical Analysis Plan (SAP) and execution of a Data Sharing Agreement (DSA). All data relevant to the study are included in the article.

Supplementary data

Supplementary data are available at *Rheumatology* online.

References

1 Ritchlin CT, Colbert RA, Gladman DD. Psoriatic arthritis. N Engl J Med 2017;376:957–70.

2 Ostergaard M, Eder L, Christiansen SN, Kaeley GS. Imaging in the diagnosis and management of peripheral psoriatic arthritis-The clinical utility of magnetic resonance imaging and ultrasonography. Best Pract Res Clin Rheumatol 2016;30:624–37.

3 Haroon M, Winchester R, Giles JT, Heffernan E, FitzGerald O. Certain class I HLA alleles and haplotypes implicated in susceptibility play a role in determining specific features of the psoriatic arthritis phenotype. Ann Rheum Dis 2016;75:155–62.

4 Chandran V, Tolusso DC, Cook RJ, Gladman DD. Risk factors for axial inflammatory arthritis in patients with psoriatic arthritis. J Rheumatol 2010;37:809–15.

5 Eder L, Chandran V, Pellet F *et al.* Human leucocyte antigen risk alleles for psoriatic arthritis among patients with psoriasis. Ann Rheum Dis 2012;71:50–5.

6 Sokolova MV, Simon D, Nas K *et al.* A set of serum markers detecting systemic inflammation in psoriatic skin, entheseal, and joint disease in the absence of C-reactive protein and its link to clinical disease manifestations. Arthritis Res Ther 2020;22:26.

7 Rahmati S, O'Rielly DD, Li Q *et al.* Rho-GTPase pathways may differentiate treatment response to TNF-alpha and IL-17A inhibitors in psoriatic arthritis. Sci Rep 2020;10:21703.

8 Sarabia S, Farrer C, Yeung J *et al.* The pattern of musculoskeletal complaints in patients with suspected psoriatic arthritis and their correlation with physical examination and ultrasound. J Rheumatol 2021;48:214–21.

9 Hao X, Yao X, Yan J *et al.* Identifying multimodal intermediate phenotypes between genetic risk factors and disease status in Alzheimer's disease. Neuroinformatics 2016;14:439–52.

10 Philip NS, Carpenter SL, Sweet LH. Developing neuroimaging phenotypes of the default mode network in PTSD: integrating the resting state, working memory, and structural connectivity. J Vis Exp 2014;89:51651.

11 Taylor W, Gladman D, Helliwell P *et al.* Classification criteria for psoriatic arthritis: development of new criteria from a large international study. Arthritis Rheum 2006;54:2665–73.

12 Maksymowych WP, Mallon C, Morrow S *et al.* Development and validation of the Spondyloarthritis Research Consortium of Canada (SPARCC) Enthesitis Index. Ann Rheum Dis 2009;68:948–53.

13 Terslev L, Naredo E, Aegerter P *et al.* Scoring ultrasound synovitis in rheumatoid arthritis: a EULAR-OMERACT ultrasound taskforce-Part 2: reliability and application to multiple joints of a standardised consensus-based scoring system. RMD Open 2017;3:e000427.

14 Ammitzboll-Danielsen M, Ostergaard M, Naredo E, Terslev L. Validity and sensitivity to change of the semi-quantitative OMERACT ultrasound scoring system for tenosynovitis in patients with rheumatoid arthritis. Rheumatology 2016;55:2156–66.

15 Terslev L, Naredo E, Iagnocco A *et al.* Defining enthesitis in spondyloarthritis by ultrasound: results of a Delphi process and of a reliability reading exercise. Arthritis Care Res 2014;66:741–8.

16 Ficjan A, Husic R, Gretler J *et al.* Ultrasound composite scores for the assessment of inflammatory and structural pathologies in Psoriatic Arthritis (PsASon-Score). Arthritis Res Ther 2014;16:476.

17 Kim D, Pertea G, Trapnell C *et al.* TopHat2: accurate alignment of transcriptomes in the presence of insertions, deletions and gene fusions. Genome Biol 2013;14:R36.

18 Wang L, Wang S, Li W. RSeQC: quality control of RNA-seq experiments. Bioinformatics 2012;28:2184–5.

19 Trapnell C, Williams BA, Pertea G *et al.* Transcript assembly and quantification by RNA-Seq reveals unannotated transcripts and isoform switching during cell differentiation. Nat Biotechnol 2010;28:511–5.

20 Ritchie ME, Phipson B, Wu D *et al.* Limma powers differential expression analyses for RNA-sequencing and microarray studies. Nucleic Acids Res 2015;43:e47.

21 Gu Z, Eils R, Schlesner M. Complex heatmaps reveal patterns and correlations in multidimensional genomic data. Bioinformatics 2016;32:2847–9.

22 Nugent R, Meila M. An overview of clustering applied to molecular biology. Methods Mol Biol 2010;620:369–404.

23 Kotlyar M, Pastrello C, Malik Z, Jurisica I. IID 2018 update: context-specific physical protein-protein interactions in human, model organisms and domesticated species. Nucleic Acids Res 2019;47:D581–D9.

24 Rahmati S, Abovsky M, Pastrello C *et al.* pathDIP 4: an extended pathway annotations and enrichment analysis resource for human, model organisms and domesticated species. Nucleic Acids Res 2020;48:D479–D88.

25 Brown KR, Otasek D, Ali M *et al.* NAViGaTOR: network analysis, visualization and graphing Toronto. Bioinformatics 2009;25:3327–9.

26 Moll J, Wright V. Psoriatic arthritis. Semin Arthritis Rheum 1973;3:55–78.

27 Eder L, Aydin SZ. Imaging in psoriatic arthritis-insights about pathogenesis of the disease. Curr Rheumatol Rep 2018;20:77.

28 Polachek A, Cook R, Chandran V *et al.* The association between HLA genetic susceptibility markers and

sonographic enthesitis in psoriatic arthritis. Arthritis rheumatol 2018;70:756–62.

29 Herster F, Karbach S, Chatterjee M, Weber ANR. Platelets: underestimated regulators of autoinflammation in psoriasis. J Invest Dermatol 2021;141:1395–403.

30 Garshick MS, Tawil M, Barrett TJ *et al.* Activated platelets induce endothelial cell inflammatory response in psoriasis via COX-1. Arterioscler Thromb Vasc Biol 2020;40:1340–51.

31 Herster F, Bittner Z, Archer NK *et al.* Neutrophil extracellular trap-associated RNA and LL37 enable self-amplifying inflammation in psoriasis. Nat Commun 2020;11:105.

32 Gilliet M, Conrad C, Geiges M *et al.* Psoriasis triggered by toll-like receptor 7 agonist imiquimod in the presence of dermal plasmacytoid dendritic cell precursors. Arch Dermatol 2004;140:1490–5.

33 Di Minno MN, Iervolino S, Peluso R *et al.* Hemostatic and fibrinolytic changes are related to inflammatory conditions in patients with psoriatic arthritis–effect of different treatments. J Rheumatol 2014;41:714–22.

34 Erfan G, Guzel S, Alpsoy S *et al.* Serum YKL-40: a potential biomarker for psoriasis or endothelial dysfunction in psoriasis? Mol Cell Biochem 2015;400:207–12.

35 Furer V, Levartovsky D, Wollman J *et al.* Prevalence of nonradiographic sacroiliitis in patients with psoriatic arthritis: a real-life observational study. J Rheumatol 2021;48:1014–21.